Renewable Energy 192 (2022) 361–372

Contents lists available at ScienceDirect

Renewable Energy

journal homepage: www.elsevier.com/locate/renene

Split-range control for improved operation of solar absorption cooling plants

Diogo Ortiz Machado [a, b, c], Adolfo J. Sánchez [d], Antonio J. Gallego [c], Gustavo A. de Andrade [b], Julio E. Normey-Rico [b], Carlos Bordons [c, e, *], Eduardo F. Camacho [c, e]

[a] IFRS - Instituto Federal de Educação, Ciencia e Tecnolgia do Rio Grande do Sul, Rua Alfredo Huch, 475, Rio Grande, 96201 460, Rio Grande do Sul, Brazil
[b] UFSC - Universidade Federal de Santa Catarina, Departamento de Automação e Sistemas, R. Eng. Agronômico Andrei Cristian Ferreira, Florianópolis, 88040 900, Santa Catarina, Brazil
[c] US - Universidad de Sevilla, Departamento de Ingeniería de Sistemas y Automática, Camino de los Descubrimientos, Sevilla, 41092, Spain
[d] MTU - Munster Technological University, Department of Mechanical, Biomedical and Manufacturing Engineering, Cork, T12 P928, Ireland
[e] ENGREEN - Laboratory of Engineering for Energy and Environmental Sustainability, Universidad de Sevilla, Spain

ARTICLE INFO

Article history:
Received 2 February 2022
Received in revised form
16 February 2022
Accepted 10 April 2022
Available online 29 April 2022

Keywords:
Renewable energy
Fresnel solar collector
Defocus
Absorption chiller
Solar cooling
Split-range control

ABSTRACT

This paper proposes the first application of a split-range control technique on a concentrating solar collector to improve an absorption plant production. Solar absorption plants have solar power availability in phase with cooling demand under design conditions. Thus, it is a powerful cooling technology in the context of renewable energy and energy efficiency. These plants need control systems to cope with solar irradiance intermittency, reject irradiation disturbances, manage fossil fuels backup systems and dump closed-loop thermal-hydraulic oscillations. In this work, control techniques are proposed and simulated in an absorption plant in Spain. The plant consists of a concentrating Fresnel solar collector connected to an absorption chiller. The objectives are to operate with 100% renewable solar energy and avoid safety defocus events while reducing temperature oscillations and control actuators effort. Firstly, the current available plant controllers are defined, then two modifications are proposed. The first modification is a split-range controller capable of manipulating both flow and defocus of the Fresnel collector, the second modification is a PI controller to substitute the original chiller on-off controller. The results compare, through validated models, the different control systems and indicate that using both proposed controllers reduces 94% of the sum of actuators effort and 43% of the integral of absolute set-point tracking error compared to the plant's factory pre-set controllers. The suggested controllers increase 66% of energy production and 63% of exergy production. Besides, the split-range technique can be extended to any concentrating solar collector control.

1. Introduction

Currently, electrical energy continues to be produced to a large extent by fossil fuel power plants, nuclear and other energy sources that are not renewable [1]. The use of renewable sources is essential to reduce the environmental impact caused by the use of fossil fuels [2,3]. It should be noted that of all renewable energy sources solar energy is undoubtedly the most abundant. Due to the current situation regarding global warming, governments are trying to boost electricity generation using renewable or sustainable energy sources, through agreements, in order to reduce global warming to well below 2 °C, although the objective is to limit it to 1.5 °C [4].

Solar energy faces different challenges when entering the market. The main and most important of all is to make it economical and competitive [3,5]. In order to overcome these challenges, it is necessary to improve the operation of the plant and optimize its production. However, these are improvements are increasingly complex to achieve due to the large size of current plants. Among the different solar concentrating technologies it can be found parabolic trough solar plants, concentrating tower solar plants or concentrating linear Fresnel solar plants. This article

* Corresponding author. US - Universidad de Sevilla, Departamento de Ingeniería de Sistemas y Automática, Camino de los Descubrimientos, Sevilla, 41092, Spain.
E-mail address: bordons@us.es (C. Bordons).

https://doi.org/10.1016/j.renene.2022.04.064

focuses on the development of control algorithms for linear Fresnel solar technology plants.

The operation of concentrating solar plants is based on the concentration of solar energy in a receiving pipe through which a heat transfer fluid circulates. The fluid will be heated by the solar radiation concentrated in the receiving pipe. Later this fluid, at high temperature, will be transported to use the heat and convert it into electrical energy, for example. However, linear Fresnel plants also have the capability to be installed in buildings for solar use, as is the case of the solar Fresnel plant of the Escuela Superior de Ingeniería de Sevilla (ETSI), University of Seville. A solar Fresnel plant installed on its roof takes advantage of solar energy to generate cold through the use of an absorption machine. This cold is used for the air conditioning of the building during hot seasons.

The main objective of the control systems in solar plants is to track a reference temperature at the outlet of the solar field. That is, to follow an optimal nominal temperature set by the operators to maximize the plant's performance. This optimization is not an easy task because solar plants are, in general, highly nonlinear and distributed processes that present significant transport delays and depend on the size of the plant. The plant complexity is a challenge to design advanced controllers to optimize production and operation.

The studies carried out on the control of the outlet temperature of solar fields are numerous such as [6] where an adaptative Model Predictive Control (MPC) strategy is designed for the Fresnel solar plant located at the ETSI, Seville. An unscented Kalman filter is used as a state estimator of the metal-fluid temperature profiles and effective solar radiation. Results are compared with a PID + feedforward control and a Generalized Predictive Control (GPC). Results showed that the proposed adaptative MPC outperformed these two strategies in temperature tracking and disturbance rejection.

The development of fuzzy incremental controller on a small-scale linear Fresnel reflector solar plant is presented in Ref. [7]. Authors used an ant colony algorithm for an optimal tuning of a PID + feedforward controller parameters to compare the proposed PI-like fuzzy incremental algorithm. Results of the Fresnel plant shows that the proposed PI-fuzzy like algorithm outperforms the conventional PI algorithm in terms of the time response metrics. The work presented in Ref. [8] presents a two layer control strategy for temperature tracking and disturbance rejection of a solar Fresnel plant. The first layer is a nonlinear MPC for regulating the outlet temperature of the solar field, while the second layer is a fuzzy algorithm for the adequate operation mode considering the operation conditions.

Other works analyzed the optimization of the solar fields, as in Ref. [9] where authors present a study on the optimization of the solar multiple[1] when designing linear Fresnel solar fields of direct generation. This work is a case study of a 50 MW Fresnel plant to find the optimum of the solar multiple. An economic optimization is used to determine the lowest Levelized Cost of Electricity (LCOE). Authors come to the conclusion that a Fresnel plant without Thermal Energy Storage (TES) should have a solar multiple of 1.7 while if it has a TES system the field should be greater with a solar multiple of 2, for 2 h energy storage. In this sense it is logical to assume that solar concentrating solar plants will need to defocus the solar field mirrors under normal operation. Therefore, control techniques as the proposed split-range that considers a proportional focus in the process control layer [11], instead of on-off defocus on the safety layer, would provide operation advantages.

[1] Solar multiple is defined as the ratio between the thermal power produced by the solar field (generator) at the design point and the thermal power required by the power block (consumer) at nominal conditions [10].

In general, concentrating solar plants must start and stop every day. The start-up is done during sunrise. Plants can use a gas burner to start-up the plant, since they must start the turbine that has been cooling overnight. In the same way, the ETSI solar Fresnel plant has a natural gas burner to pre-heat the entire circuit as well as the absorption machine to start working. However, the use of gas is not the most convenient strategy when operating renewable plants and even more if we are talking about solar renewable energy.

The previous heating of the solar field as well as the absorption machine is crucial for the operation of the plant, since the operation of the absorption machine must be carried out in a very narrow temperature range [12], around 160[$^{\circ}C$]. This article shows how the plant begins to work thanks to the use of the gas burner. However, if the heating of the circuit is carried out in an uncontrolled way, it can cause oscillations in the outlet temperature that will be maintained over time, since initially the entire system is cold and by increasing the flow-rate through the pipes, the cold flow will be moving towards the solar field. It will take a while for the entire circuit to be homogeneous at nominal temperatures. As long as this does not happen, there will be temperature fluctuations caused by the mass transport of water. These temperature oscillations are fed back as it is a closed circuit and will cause the system to continuously activate and deactivate the absorption machine several times since it would be leaving the nominal operating temperature of the absorption machine and the operating mode must be changed [8]. In addition to changing the operating mode of the absorption machine, it would also be consuming gas again to try to raise the internal Lithium-Bromide temperature. However, the use of gas is a resource that could be eliminated if a controlled start-up to heat the pipes and the absorption machine were made. This would not only reduce the cost of the bill caused by the use of gas but also in the installation of the plant itself, since it would not be necessary to invest in the installation of a gas burner. Starting the plant with gas becomes a difficult decision, if later it may turn out that the day turns cloudy and it would not be possible to operate anymore, in which case gas and money would have been wasted, something that will not happen if only the solar resource is used.

In this paper, a split-range controller on the Fresnel and a PI controller on the High Temperature Generator (HTG) of the absorption machine are proposed on the ETSI absorption plant. The objective is to avoid the use of natural gas in the start-up as well as to avoid possible safety defocusing actions. The HTG controller will be in charge of reducing the oscillations of the plant as well as the control effort, while the strategy based on the split-range controller will be in charge of accelerating the start-up of the plant without using natural gas. The split-range controller will be able to accelerate the process avoiding overheating, which translates into an improvement in the stability of the plant and consequently an increase in production. In addition, the split-range controller will take into account that the flow rate is the main manipulated variable, at least until it reaches saturation, at which point the flow rate will be at its maximum and the split-range controller must begin to manipulate the defocus to control the outlet temperature.

The rest of the paper is organized as follows: Section 2 describes the process and the operation of the ETSI Fresnel absorption plant. In Section 3 the inherited factory pre-set and revamp control schemes are presented and simulated to motivate this paper controllers proposals of Section 4. Plant models details, simulations plans, and the results are presented in Section 4. Section 5 draws the paper to an end with some conclusions.

2. ETSI solar absorption plant and control premise

The purpose of solar plant studied in this work is to reduce non-renewable energy consumption and avoid carbon dioxide (CO_2)

emissions. Its objective is to generate chilled water through an absorption chiller using hot water from a concentrating solar collector. The chilled water is fed to the ETSI building in order to supplement the heat ventilation and air conditioning (HVAC) system [12].

Table 1 organizes the main characteristics of the plant. The absorption chiller worked with a daily average cooling power of 135 kW, with a worst-case of 70 kW, and a Coefficient of Performance (COP) between 1.1 and 1.25 in a campaign of five days of operation during the cold demand season [12]. Equation (1) calculates the Solar Heat Fraction (SHF) where Q_{solar} is the energy generated in the solar collector and Q_{gen} is the energy used in the absorption machine

$$SHF = \frac{Q_{solar}}{Q_{gen}}, \tag{1}$$

that results in 0.75 from operational data. This means that 75% of injected heat in the chiller was from the solar resource and the other 25% came from gas burning [12].

The problem is that the purpose of the solar cooling plant is to reduce non-renewable energy consumption and avoid carbon dioxide emissions. The authors in Ref. [12] investigate the ETSI absorption plant trade-off between burning gas, CO_2 generation, and costs, performing an economic and CO_2 emission analysis and comparing the hybrid gas/solar chiller to an electric one. Table 2 updates and summarizes the analysis considering actual gas [13] and electricity [14] costs in Spain.

Table 2 compares the performance of chillers considering a fixed output cooling generation of 1000 kWh. ETSI absorption plant hybrid operation reduces 75% of the associated cost and CO_2 emissions compared to the gas chiller. However, Table 2 shows that the electric compression chiller has lower cost and emissions than the gas absorption chiller. Therefore, it is more profitable and less pollutant to compose solar cooling with electricity instead of gas.

The ETSI building has a HVAC system equipped with electric compression chillers which is an option to avoid using the backup boiler equipped in the absorption chiller, see Fig. 1. Therefore, this paper's premise is to operate the solar absorption cooling plant only with solar energy, thus, a SHF = 1, as it seems a better strategy. Thereby, the gas boiler is not modeled or simulated in this work. The next section presents the legacy controls simulations and the motivation of this work considering the above mentioned premise.

Table 2
Comparison between electric compression, thermal absorption, a hybrid solar/gas absorption performances.

Chiller	Compression	Absorption	ETSI Hybrid Absorption	
Primary energy	electric	gas	solar	gas
COP	3,50	1,10	1,10	
Energy output [*kWh*]	1000,00	1000,00	1000,00	
Energy input [*kWh*]	285,71	909,09	681,82	227,27
Input cost [*euro*/*kWh*]	0,17	0,07	0,00	0,07
Associated cost [*euro*]	49,59	66,55	0,00	16,64
CO_2 emissions [*kg*/*kWh*]	0,26	0,19	0,00	0,19
Associated CO_2[*kg*]	74,29	176,36	0,00	44,09

3. Motivation

This paper proposes new control techniques to enhance the ETSI solar absorption plant operation. Fig. 1 depicts the plant schematic where each fluid stream has a label from 1 to 12. The plant comprises the Fresnel collector as the solar heat source, the absorption machine as the heat sink, long pipes that connects both processes, and a valve that can route the water streams. Note that the absorption machine's evaporator generates the cooling effect, which is delivered to the HVAC system by streams 9 and 10.

The objective of Controller C1 is to supply the HTG with water at appropriate temperature by regulating the solar collector outlet temperature T_2 through manipulating the mirror focus f, or the pump flow q. The objective of Controller C2 is to regulate HTG lithium-bromide solution temperature T_8 of the absorption machine by manipulating valve aperture v. The Fresnel collector inlet stream 1 is the stream 7 after flowing through the pipe. And the stream 7 is a mixture of the HTG outlet stream 6 and the valve bypass stream 4. Therefore, the process is a hydraulic closed loop. This thermo-hydraulic system has complex dynamics such recycle [15] that could arise integrating snow-ball effect [16,17], dead-times, because mass transfer across long pipes [18], and resonance modes [19], that leads to strong non-linearities and oscillations reported in Ref. [12], and in measurement data. Next, plant simulations illustrate the oscillations considering the legacy controller of the plant, and discusse the operation issues and

Table 1
ETSI Solar Absorption plant characteristics.

Fresnel collectors	
Solar field aperture	352 m^2
Absorber tube length	64 m
Absorber tube model	SCHOTT PTR 70
Heat transfer fluid	Saturated liquid water
Operation temperature (max)	180 °C
Operating pressure	13 bar
Mirror reflectivity	0.92
Pipelines	
Inner diameter of pipeline	0.052 m
Total solar circuit length	365 m
Absorption chiller BROAD-BZH15	
Cooling capacity	174 kW
COP	1.34
Temperature evaporator inlet	12 °C
Temperature evaporator outlet	7 °C
Evaporator flow rate	30 m^3/h
Temperature condenser inlet	30 °C
Temperature condenser outlet	37 °C
Condenser flowrate	37 m^3/h
Fuel	Natural gas
HTG Temperature	145 °C

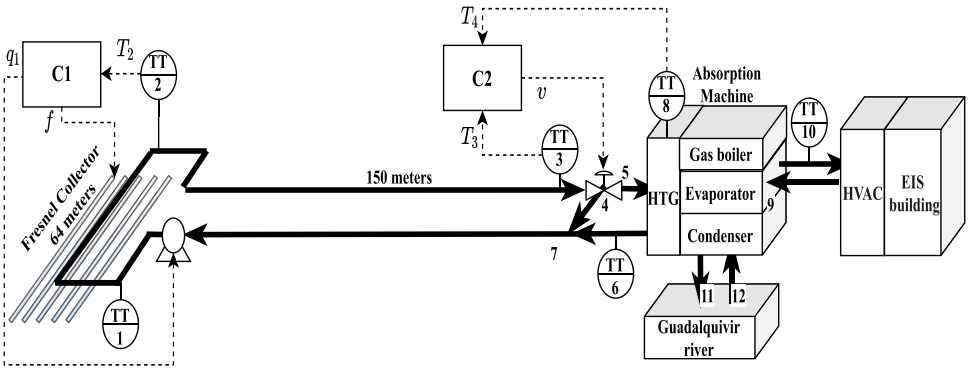

Fig. 1. General schematic of the absorption plant in the *Escuela Tecnica Superior de Ingenieria (ETSI)* in Seville University.

opportunities. This work considers the absorption chiller model and the Fresnel solar collector model described and validated in Ref. [8], and [20], respectively.

There are two inherited control strategies implemented in the Fresnel's hardware and one implemented on the chiller hardware. The original Fresnel control rules running on controller C1 are described in Equation (2).

$$\begin{cases} q_1 = 0, & \text{if } I \leq 250, \\ q_1 = 12, & \text{if } I > 250, \\ f = 0, & \text{if } q_1 = 0, \\ f = k_{p1}\left(e_1(t) + \int \frac{1}{t_{i1}} e_1(t)dt\right), & \text{if } q_1 = 12, \end{cases} \tag{2}$$

where $q[m^3/h]$ is the flow, $I[W/m^3]$ is sun irradiance, f is the mirror 's focus with a range from 0 to 1, k_{p1} is the proportional gain of controller C1, t_{i1} is the integral time of controller C1, $e_1(t) = T_{sp2} - T_2(t)$ is the error between the desired set-point, $T_{sp2} = 170[^\circ C]$, and the outlet temperature, T_2 of controller C1. The first Fresnel controller has an on-off flow manipulation with $q_1 = 0$ when the irradiance is below a minimum value, and $q_1 = 12[m^3/h]$ when the irradiance is sufficient to start the plant, the latter condition allows manipulating the focus with a proportional plus integral (PI) law. The original Fresnel controller (C1) performance is depicted on Fig. 2.a and 2.c. C1 starts the pump at 9:00 considering a clear sky irradiance profile (yellow line) of Fig. 2.b. Then, the PI controller starts regulating the outlet temperature T_2 by manipulating the mirrors focus when the flow is at maximum and $I > 250$, accordingly to Equation (4). This phase is called preheating and recirculates water between the collector and chiller valve with full focus until T_3 reaches a predefined temperature starting the chiller.

$$v = \begin{cases} 1, & \text{if } T_3 > 160 \text{ and } T_8 < 135, \\ 0, & \text{if } T_3 \leq 160 \text{ or } T_8 \geq 145. \end{cases} \tag{3}$$

Controller C2 is responsible for starting the absorption chiller, the original control rules are described in Equation (3). Where $v = [0, 1]$ is the three-way valve opening, when $v = 1$ it is feeding the chiller, when $v = 0$ it is by-passing the chiller, T_3 is the valve inlet temperature, and T_8 is the HTG temperature. Note that the chiller factory pre-set C2 is an on-off controller with hysteresis that seeks to maintain the HTG temperature inside a band between the lower temperature set-point $\underline{T}_{sp8} = 135$ and the upper temperature set-point $\overline{T}_{sp8} = 145[^\circ C]$, see Fig. 2.b.

The plant simulation considering the factory pre-set C2 is depicted in Fig. 2.b and 2.d. When the HTG inlet temperature T_3 reaches a predefined temperature $T_{sp3} = 160[^\circ C]$ and the internal HTG temperature T_8 is below $\underline{T}_{sp8} = 135[^\circ C]$ the controller opens the valve aperture v and feeds the HTG, both events happen at 13:00 on Fig. 2.b and Fig. 2.d, respectively. Then, T_8 reaches $\overline{T}_{sp8}$ and the valve closes, decreasing the HTG temperature. The problem is that when T_8 drops below $\underline{T}_{sp8}$ again, the valve does not open owing to $T_3 < 160$, because the first valve aperture itself decreases the water temperature inside the pipes and, ultimately, T3. If T_8 stays below $\underline{T}_{sp8}$ for more than 30 min after the start-up, the boiler start burning gas. Fig. 2 shows that the boiler would burn gas between 13:00 and 14:00. The gas backup heat effect is not seen because the premise of this work of not using the boiler and, therefore, the boiler is not simulated.

Note that just before the valve opens at 13:30, T_3 and T_8 are at temperature of 160 and 75[°C], respectively. Thus, when the valve opens, the internal water, that was inside the HTG at 75[°C], enters in the pipes with water at 160[°C], generating a temperature gradient of 85[°C]. Then, both low and high temperature water plug flows travel inside the pipes concomitantly which reflects the oscillatory temperatures depicted on Fig. 2.a. Note on Fig. 2.a that the C1 cannot stabilize T_2 even with strong focus actuation effort depicted on Fig. 2.c. It is also worth noting on Fig. 2.a that the temperature oscillations have a minimum of T_8, and a maximum of T_3 at 13:00, just before start feeding the HTG. Note that the oscillations periods are coincident with the pipes hydraulic residence time, $\tau = (V_{fresnel} + V_{piping})/q_1$. In other words, the period of temperature oscillations on Fig. 2.a is the time that the cold plug flow takes to make one lap on the hydraulic circuit concerning the temperature transmitter TT2 position. Resuming, the factory pre-set control strategy leads to temperature gradients, strong focus actuation and boiler gas burning.

These results show that even though the factory pre-set control does not trigger safety total defocus, a security control to prevent overheating, the factory pre-set control leads to bad reference tracking of both Fresnel and HTG temperatures, and a strenuous effort of the solar tracking device, which results in premature wear of the focus mechanism. In practice, a second controller was implemented in the plant's hardware to reduce the focus mechanism wear, and also to reduce solar energy rejection [21].

The second Fresnel controller C1, henceforth called revamp control, exchange the focus proportional manipulation to flow proportional manipulation, and it is described by Equation (4). Focus manipulation is on-off with $f = 0$ when the irradiance is below a minimum value, and $f = 1$ when the irradiance is sufficient

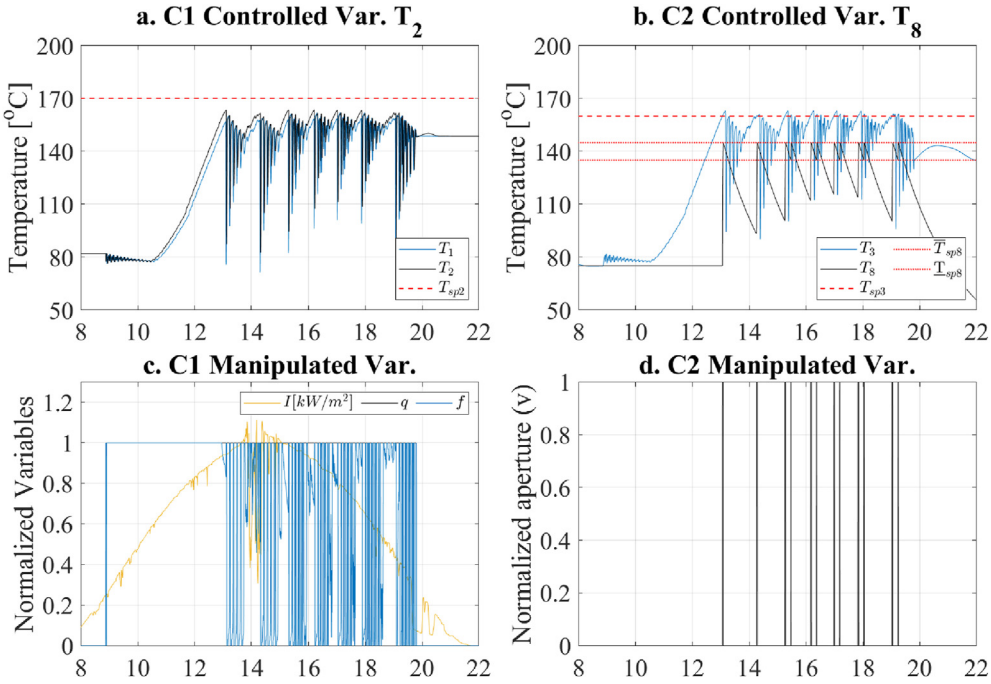

Fig. 2. Original factory pre-set control performance on Scenario 1 (S1).

to start the plant. The latter condition allows using a PI law with proportional flow q_1 range from 2 to 12$[m^3/h]$. The revamp Fresnel's controller performance is depicted on Fig. 3.a and 3.c.

$$\begin{cases} f = 0, & \text{if } I \leq 250, \\ f = 1, & \text{if } I > 250, \\ q_1 = 0, & \text{if } f = 0, \\ q_1 = k_{p1}\left(e_1(t) + \int \frac{1}{t_{i1}} e_1(t)dt\right), & \text{if } f = 1. \end{cases} \tag{4}$$

The revamp controller performance depicted on Fig. 3 has faster

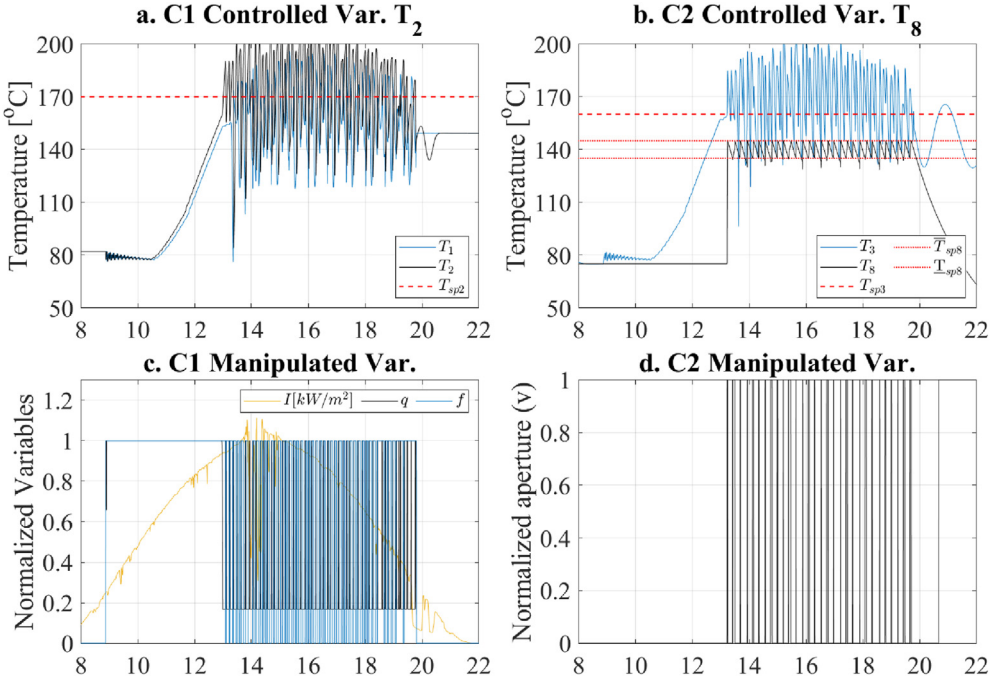

Fig. 3. Revamp control performance on Scenario 2 (S2).

start-up than the factory pre-set control due flow manipulation capability. The revamp controller regulates the HTG temperature T_8 avoiding burning gas. Although it has qualitatively worst gradient temperature and oscillations than the factory pre-set controller. Note that the focus has actuation on 3.c despite not having low irradiance. This is because the Fresnel's safety defocus device described by Equation (5).

$$f_s = \begin{cases} 1 & \text{if } T_2 \leq 160[^\circ C], \\ 0 & \text{if } T_2 \geq 190[^\circ C]. \end{cases} \tag{5}$$

Thus, the Fresnel solar collector has a safety full defocus system which overrides the process controller. The safety action cools the outlet temperature from an abnormal outlet temperature of 190[°C] to 160[°C]. Fig. 3.b depicts the revamp controller safety full defocus events (blue line).

Resuming, both simulations of inherited factory pre-set control and revamp control of the ETSI absorption plant show strong oscillatory behaviour and poor set-point tracking disregarding the gas boiler operation. On the one hand the factory pre-set control advantage is that it does not have safety defocus events, although, it has disadvantages as it does not track the HTG temperature set-point properly, would start the gas boiler, has a slower start-up ramp, and cause solar energy rejection. On the other hand the revamp control advantages is that it tracks the HTG temperature setpoint, would not burn gas, have a faster start-up, although, it presents safety defocus actuation as draw-back. Therefore, the controllers have complementary advantages. The following section proposes combining the advantages and suppressing the disadvantages of inherited controllers in a new control proposal to enhance the plant performance.

4. Proposed controls

Firstly, this work proposes using a proportional plus integral (PI) law on the chiller controller C2 on Section 4.1. It is expected that the PI controller would lead to both reduction of oscillations and Fresnel's actuators effort. Secondly, this work proposes using a split-range advanced control technique on the Fresnel controller C1 on Section 4.2. It is expected that using both flow and focus in the same PI controller scheme would combine the fast start-up performance of manipulating the flow with the extended controllability of using the focus proportionally. The latter ultimately will avoid unnecessary solar energy rejection and safety full defocus events. The results of the two solutions together would avoid gas burn and safety defocus events while stabilizing operation, and increasing energy production.

4.1. High Temperature Generator controller

The HTG inlet temperature T_3 comes from the Fresnel solar collector outlet temperature T_2 through the pipes and vice versa. The problem is that the factory controller has an on-off law that generates strong oscillations a temperature gradients in the plant. Therefore, it is proposed the proportional plus integral control (PI) law described in Equation (6).

$$v = k_{p2}\left[e_2(t) + \frac{1}{t_{i2}}\int e_2(t)dt\right]. \tag{6}$$

where k_{p2}, t_{i2}, and $e_2(t)$ are the proportional gain, integral time, and error of controller C2. The error is calculated as $e_2(t) = T_{sp8} - T_8(t)$, it is the difference between the desired set-point, $T_{sp8} = 145[^\circ C]$, and the outlet temperature, T_8 of controller C2. The control law was discretized using a backward Euler technique, and its was tuned using trial an error, the same tuning is used in all controllers and simulations.

4.2. Split-range controller on concentrating solar collectors

A split-range controller is functional when there are two or more manipulated variables associated with a controlled variable. It is typically applied to extend the controller's steady-state range by switching the primary actuator when it becomes saturated [22]. Therefore, concentrating Fresnel solar collectors are typical processes where the split-range advanced control can improve operation. Specifically, the ETSI Fresnel automated system is capable of manipulating the flow and the mirror's focus, therefore, implementing a split-range controller. Selecting the flow as the primary manipulated variable seems logical because it actuates in absorbing the solar heat that has already entered the receiver. The focus is the secondary manipulated variable because it operates rejecting the solar irradiance and wasting energy. In other words, the flow will absorb the maximum solar incident energy on the solar field until saturation; then, the defocus will act because it is the only manipulated variable capable of affecting the outlet temperature. Fig. 4 depicts the split-range schematic on the Fresnel solar collector.

Equations (7) and (8) describe this controller. It is worth noting that the control law is the well known PI with an internal output signal u_1 chosen to vary from 0 to 100. The splitter divides signal u_1 between both actuators as depicted on Fig. 5. The problem here is that the flow and focus must have inverse proportional gain signal because increasing the focus will increase T_2, while increasing the flow will decrease T_2. A positive and a negative slope of the linear equations depicted on Equation (8) solve this question, which Fig. 5 exemplifies geometrically. Note that the manipulated variables ranges used in simulations are from 2 to 12[m^3/h] for the flow and from 0 to 1 for the focus.

$$u_1 = k_{p1}\left[e_1(t) + \int \frac{1}{t_{i1}} e_1(t)dt\right]. \tag{7}$$

$$\begin{cases} q_1 = 2 + 0.2u_1, & 0 \leq u_1 \leq 50; \\ f = 1 - 0.02(u_1 - 50), & 50 < u_1 \leq 100. \end{cases} \tag{8}$$

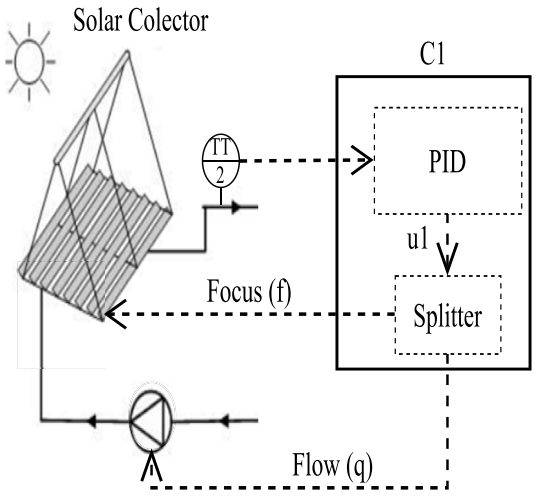

Fig. 4. Split-range block diagram on the Fresnel solar collector.

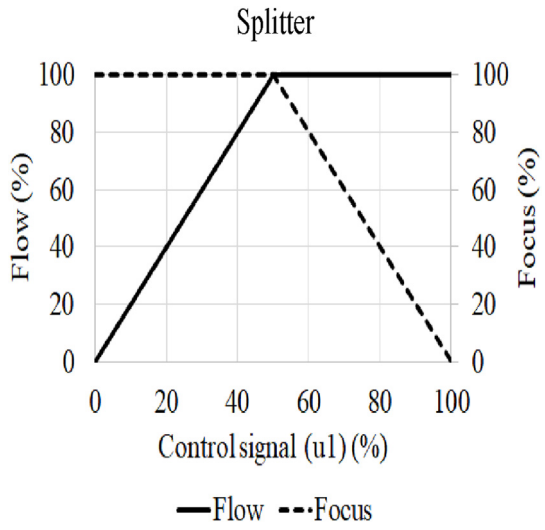

Fig. 5. Split range signal scheme.

The mirror focus will reduce from its maximum only when the pump saturates, that is, when it becomes impossible to increase sun heat absorption through the flow. Therefore, this solution increases thermal energy production since the focus reduction is sufficient to follow the temperature reference with minimum solar energy rejection. In practice, the split-range technique merges the factory pre-set and revamp controllers ideas of the IES plant. It has the advantage of using the flow to maximize energy production and focus on maintaining the controllability of the outlet temperature.

To summarize, the split-range is the most straightforward and advanced control technique capable of manipulating the flow and defocus together. It has an active defocus already in the process control automation layer contributing to avoiding safety total defocus action of the safety automation layer.

5. Simulation studies

This section is divided in four subsections approaching the mathematical model of the solar cooling plant, the simulation cases, the performance indexes and the results.

5.1. Mathematical model of the solar cooling plant

This work uses the absorption machine model described in Ref. [8], which was validated with real data and demonstrated that it is a good representation of the real process. The model consists of three parts: the high-temperature generator (HTG) connected to the solar collector, the condenser connected to the Guadalquivir river, and the evaporator connected to the ETSI building through the HVAC system. Each sub-model is a lumped parameter model.

The Fresnel solar collector subsystem is composed by two parts where a phenomenological distributed parameters model describes each. Equation (9) describes the metal tube, and Equation (10) describes the water flow.

$$\rho_m c_m A_m \frac{\partial T_m}{\partial t} = If\eta_{opt}\eta_{geo}Gf_s - H_l G(T_m - T_a) - LH_t(T_m - T_f), \tag{9}$$

$$\rho_f c_f A_f \frac{\partial T_f}{\partial t} + \rho_f c_f q \frac{\partial T_f}{\partial x} = LH_t(T_m - T_f), \tag{10}$$

where m and f sub-indexes refer to metal and fluid, respectively. The variable $A_m[m^2]$ is the cross-section area of metal absorber pipe, $I[W/m^2]$ refers to direct solar irradiance, η_{opt} is the optical efficiency, η_{geo} is the geometric efficiency, $G[m]$ is the mirrors' total aperture, $H_l[W/(m^2\,^\circ C]$ is the global coefficient of thermal loss, L $[m]$ is the absorber pipe length, and $H_t[W/(m^2\,^\circ C]$ is the coefficient of heat transmission between metal and fluid. The proportional mirrors focus f, and the safety full defocus f_s were added to the model to evaluate the effect of this actuator. While the first can vary the concentrated solar energy density on the receiver with values between 0 and 1, the latter has a discrete state of 0 or 1. For heat transfer coefficients, material properties, validation, and further model details, refer to Ref. [20]. Equations (9) and (10) were discretized in space and in time to be solved in integration steps of 15 $[s]$.

The piping system is an essential part of the IES plant. The tubes connect the systems and have an appreciable length. Note that the total solar circuit length is 365$[m]$ where only 64$[m]$ is composed by the Fresnel absorber length. Therefore, the piping is not negligible in the dynamics of this plant because of hydraulic recycle, snowball effect, dead-times, resonance modes, and tube-water mass thermal accumulation between the chiller and the solar collector. The thermal capacitance of the piping system is 82% of the total circuit. Thus, the tubes' accumulated energy affects the plant operation. The piping models are the same as the ones in Equation (9), and (10), but with different ambient losses and null solar input terms.

The valve is a three-way, electrically actuated, with proportional regulation capacities. This valve can change the plant operation from recirculating to feeding the HTG and vice-versa. The valve is modeled as a flow splitter and mixer system based on the energy and mass conservation laws. The valve itself is a splitter that has one mass input and two outputs modeled by Equation (11) and Equation (12), respectively,

$$q_5 = vq_3, \tag{11}$$

$$q_4 = (1 - v)q_3. \tag{12}$$

The Fresnel inlet flow comes from the mixer point, calculated as $q_7 = q_4 + q_6$. The dynamics of the thermal processes are appreciably slower than the actuators. Thus the modeling considers that the pump and the valve actuators are instantaneous.

5.2. Simulation cases

Two different irradiation profiles, depicted in Fig. 6, are considered to contrast the controllers' performance.

For the study, twelve scenarios were considered, as depicted in Table 3. They are obtained combining the three different control strategies in C1 and two different controllers in C2, and the two irradiation profiles.

Simulations S1 to S3 use the C2 on-off controller. Simulation S1 considers C1 controller with fixed flow and variable focus. Simulation S2 uses C1 controller with proportional flow and fixed focus, while simulation S3 depicts the split-range controller C1, proportionally manipulating both flow and focus. Simulations S4 to S6 consider the respective C1 control laws of S1, S2, and S3 but with the PI control law on C2. Simulations S1 to S6 consider the clear day irradiation profile of Fig. 6.A, were simulations S7 to S12 have the same combinations of controllers C1 and C2 as mentioned in S1, S2 and S3, but considering the cloudy sky irradiation profile of Fig. 6.B. The initial conditions are based on the normal conditions of the plant after the night considering that the plant worked the day before. The initial pipes temperature is 80$[^\circ C]$ because ambient heat losses of the processes and pipes during the night drops the

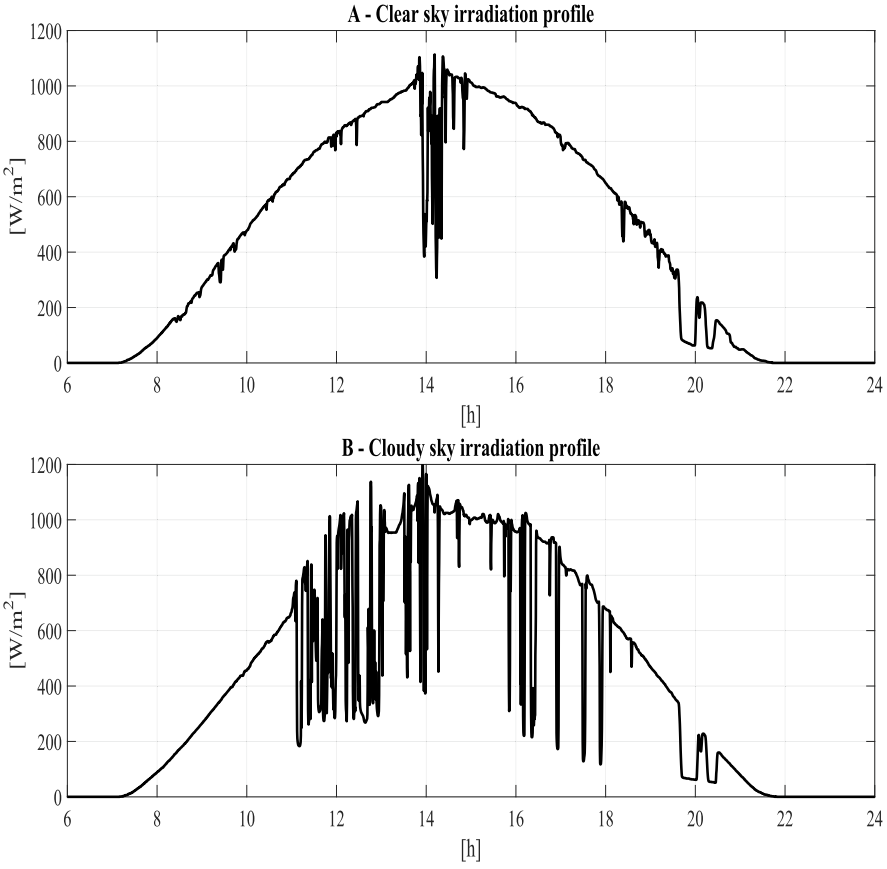

Fig. 6. Local solar irradiation measurements. A - Clear sky irradiation profile of June 09, 2009. B - Cloudy sky irradiation profile of June 26, 2009.

Table 3
Simulations scenarios. C1: PI-Focus (Equation (2)), PI-Flow (Equation (4)), PI-Split-Range (Equation (8)). C2: on-off (Equation (3)), PI (Equation (6)).

Simulation		I	C1	C2
S1	Factory	90A - clear sky	PI - Focus	on-off
S2	Revamp		PI - Flow	on-off
S3	Improved1		PI - Split-range	on-off
S4	Improved2		PI - Focus	PI
S5	Improved3		PI - Flow	PI
S6	Proposal		PI - Split-range	PI
S7	Factory	90B- cloudy sky	PI - Focus	on-off
S8	Revamp		PI - Flow	on-off
S9	Improved1		PI - Split-range	on-off
S10	Improved2		PI - Focus	PI
S11	Improved3		PI - Flow	PI
S12	Proposal		PI - Split-range	PI

temperature 80[$^\circ C$] during 12:00[h] [12].

5.2.1. Performance indexes

This section defines indexes used to compare the control strategies of each simulation case depicted in Table 3. The indexes quantifies safety full defocus events, gas boiler trigger use, operation time, and production performances. Note that this work premise is not using gas. Therefore, the gas boiler trigger is a detection of the condition where the absorption chiller would start burning gas, and not the boiler simulation. The boiler trigger BT is a boolean variable. In other words, it gives a measure if a given control system fulfills, or not, the condition of not burning gas.

The control performance indexes are the Normalized Cumulative Actuator Effort (NCAE) [23], the Integral of Absolute Error (IAE) of temperature control, and gas boiler trigger ($BT = 0, 1$), which is 1 if the controller is not capable of maintaining the HTG temperature in the set-point 30 min after HTG start-up.

Equation (13) describes the actuator effort for a generic manipulated variable u

$$NCAE = \frac{1}{\delta u} \sum_{k=1}^{N} |\Delta u|, \tag{13}$$

where $\delta u = u_{\max} - u_{\min}$ is the manipulated variable range, N is the total number of samples in the simulation time considering $I \geq 250$

$[W/m^2]$, thus, sufficient irradiance power for plant operation, $\Delta u = u(k) - u(k-1)$ is the control increment, and $u[k]$ is the manipulated variable value in sample time k.

Equation (14) is the Integral of Absolut Error (IAE) used here to measure the tracking and disturbance rejection responses of the closed-loop control system considering the error as $e = y_{sp} - y$ of a generic controlled variable y

$$IAE = \sum_{k=1}^{N} |e(k)|. \tag{14}$$

The safety performance index is the number of full defocus events N_{fs} that occur according to the conditions of Equation (5). The operation time t_{op} is defined to evaluate the start-up effect on plant production. It is the time of the chiller operation during the simulation. Note that the lower the start-up time, the greater the chiller operation time considering the same sundown time.

The production performance indexes are the total energy production E and total exergy production X. The energy production is given by Equation (15)

$$E = t_s \sum_{k=1}^{N} q_{10}(h_{10}(k) - h_9(k)), \tag{15}$$

where t_s is the sampling time, $h = cT[J/kg]$ is the specific enthalpy, which is the product of the specific heat capacity $c[J/(kg^{\circ}C)]$ and the stream temperature $T[^{\circ}C]$.

Exergy is the measure of the departure of the state of the system from that of environment, therefore, it is attributed to both, the system and the environment [24]. Exergy is a concept that indicates the energy quality considering its transformations and different natures. Despite exergy having more than one hundred years of existence just in the later years it has been applied to heat and cooling policies with focus in increasing efficiency [25,26]. The total exergy production is given by Equation (16) [24].

$$X = t_s \sum_{k=1}^{N} q_{10}(x_{10}(k) - x_9(k)), \tag{16}$$

where $x = c(T - T_0 - T_0 \ln(T/T_0))$ is the specific exergy, and $T_0[^{\circ}C]$ is the ambient temperature.

5.3. Results - clear sky scenario

Fig. 7 depicts Scenario S6 results considering the proposed controllers. It is evident that the proposed solution leads to an expressive plant stability enhancement if compared to the inherited controls shown in Figs. 2 and 3. In addition, both C1 and C2 track T_{sp2} and T_{sp8}, C1 does not have any total safety defocus event, and C2 would not burn gas. Fig. 7.c shows that the Fresnel controller imposes a low flow and high focus from 9:00 to 13:00, resulting in a fast start-up of the plant presented in Fig. 7.a. At 13:00, the Fresnel inlet temperature T_1 has a fall disturbance rejected by the flow, according to Fig. 7.c (black line). Fig. 7.d shows that the chiller valve opening at almost 13:00, together with the T_8 and T_3 difference, propagates in the pipes and causes T_1 disturbances. It is worth noting in Fig. 7.b that the valve opens because of $T_3 \geq T_{sp3}$. The PI law implemented on C2 has a critical impact on smoothing v, T_8, and T_1, resulting in a whole plant stable operation. The split-range law implemented on C1 has pivotal importance on controlling T_2 and avoiding overheating the solar collector. It is worth noting in Fig. 7.a that $T_1 > T_{sp2}$ just before 14:00. The inlet temperature above the outlet set-point temperature means that the flow loses its controllability, since increasing the flow will not decrease the outlet temperature. Regardless of the flow limitation, Fig. 7.c shows that the split-range controller switches from the saturated flow to the focus as manipulated variable, rejecting irradiance disturbances at 14:00, and decreasing T_2 to the set-point.

Table 4 resumes the performance of scenarios S1 to S6 regarding a clear sky irradiation case. Simulation S1 to S3 uses the original on-off control on C2. Note that Fig. 2, and Fig. 3 show S1 and S2 performances. Table S1, columns N_{fs} and BT, show that the split-range implementation on C1 (S3) does not trigger the boiler as S1 while reducing the defocus events compared to S2. However, scenario S3 shows that C1's split-range control in combination with the on-off control on C2 is insufficient to operate the plant without safety defocus events. In this sense, S1 to S3 controls are unsuitable because neither fulfill the premise of not burning gas and operating without triggering the safety defocus.

Note in Table 4 that scenarios S4 to S6 have $BT = 0$. Thus, implementing the PI on C2 avoids triggering the boiler in all scenarios. Although, Scenario S5 presents safety defocus events indicating that modifying exclusively the PI on C2 is also not sufficient to operate the plant without full defocus events. Furthermore, S5 has the most intensive $NCAE$ and the worst performance of IAE, E_{evap} and X_{evap}. This performance occurs because manipulating only the flow is insufficient to decrease Fresnel's outlet temperature. Therefore, T_2 reaches the high safety threshold, triggering safety total defocus, generating oscillations, and poor plant performance.

The two scenarios that do not trigger the boiler and do not have safety defocus events in Table 4 are S4 and S6. A further comparison between S6 and S4 shows that S6 has a IAE_T of 9.54×10^4 while S4 of 1.08×10^5, thus S6 has a total IAE_T reduction of 11%. Where IAE_T is the sum of IAE, $IAE_T = IAE_{C1} + IAE_{C2}$. Scenario S6 presents a total $NCAE_T$ of 10.11 while Scenario S4 of 17.48, a reduction of 42%. Where $NCAE_T$ is the sum of $NCAE$, $NCAE_T = NCAE_q + NCAE_f + NCAE_v$. Furthermore, Scenario S6 presents an energy and exergy production increase of 9% compared to S4. Such enhancements are due to the split-range controller used on the Fresnel, since S4 and S6 use the same PI controller in the chiller. The split-range controller impose a low flow in the Fresnel at the dawn and sundown, resulting in faster start-up and a delayed shut-down, increasing chiller time of operation t_{op}, see Fig. 7.c. The factory pre-set controller, in its turn, is not capable of proportionally manipulating the flow. Therefore it takes more time to reach T_{sp2}, having a lower t_{op}. Thus this work finds a trade-off between preheating time and initial accumulated energy in the hydraulic loop with energy production and plant stability. The more preheating phase accumulates, the more stable the start-up and the following operation of the absorption machine will be. The problem is that prolonged thermal accumulation in the hydraulic loop leads to a delayed chiller start-up, shortening its operation time and reducing production.

Comparing the proposed control evaluated on scenario S6 with the factory pre-set control simulated on scenario S1 indicates that the proposed controller has 43% IAE_T reduction, 94% $NCAE_T$ reduction, and 66% and 63% of energy and exergy production increase. Therefore, the Fresnel collector split-range control with the HTG PI control does not burn gas or has safety defocus, resulting in the best overall control performance of Table 4.

5.4. Results - cloudy sky scenarios

Fig. 8 depicts scenario S12 which describes the proposed controller results. Note that the proposed controllers can reject disturbances and track set-points of the plant in the case of a cloudy sky irradiance. The proposed controllers have the same overall performance as presented in Fig. 7. The difference is that Fig. 8.c highlights the split-range controller disturbance rejection capabilities. Note that C1 manipulates the flow (black line) to reject the strong irradiance disturbances (yellow line) from 11:00 to 14:00, while the focus (blue line) is at maximum. Then, from 14:00 to

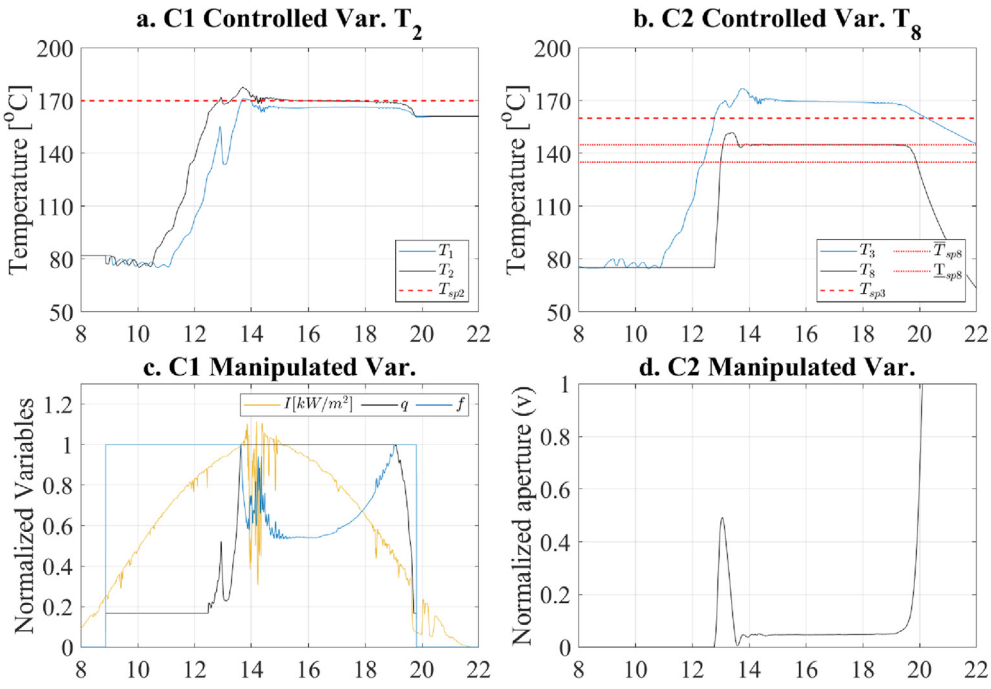

Fig. 7. Proposed Controller performance on Scenario 6 (S6).

Table 4
Scenarios performance indexes in a clear sky day.

Scenario	IAE_{C1} [°Ch]	$NCAE_f$	$NCAE_q$	N_{fs}	BT	IAE_{C2} [°Ch]	$NCAE_v$	t_{op} [h]	E_{evap} [MJ]	X_{evap} [MJ]
S1	1.47×10^5	130.09	2.40	0	1	2.53×10^4	24.00	6.58	−495.07	25.97
S2	1.51×10^5	0.00	107.34	45	0	4.43×10^2	58.00	6.41	−653.46	33.06
S3	1.16×10^5	165.86	105.41	3	0	4.32×10^2	72.00	6.86	−771.07	38.85
S4	1.08×10^5	13.55	2.40	0	0	1.12×10^3	1.53	6.58	−752.02	38.82
S5	1.38×10^5	0.00	103.22	41	0	8.45×10^3	7.82	6.41	−707.53	36.64
S6	9.54×10^4	4.82	3.25	0	0	2.20×10^3	2.04	6.86	−822.33	42.33

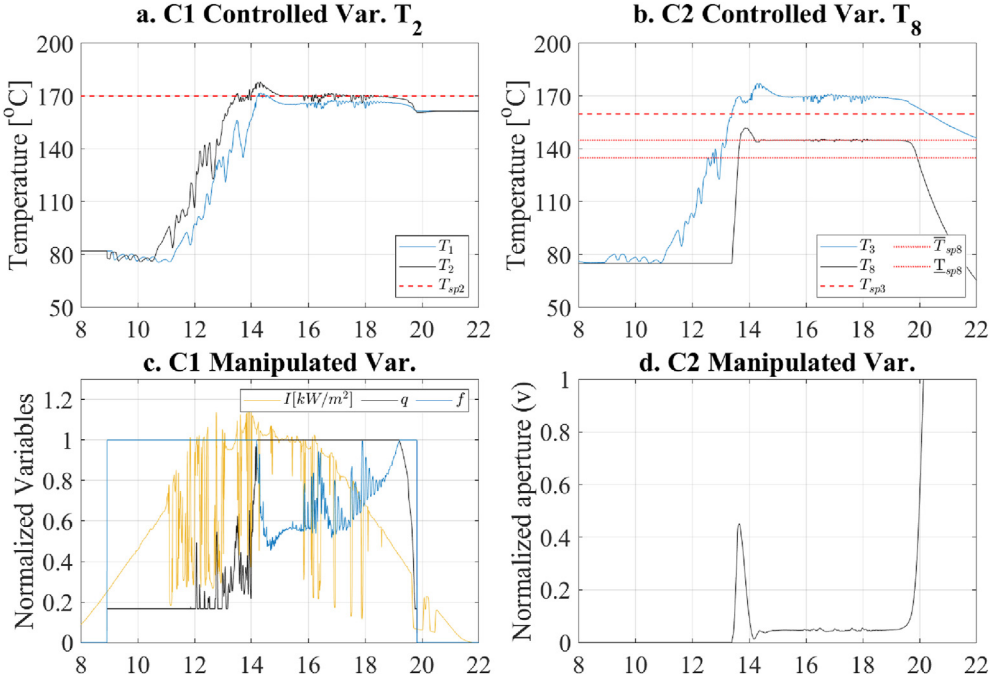

Fig. 8. Proposed Control performance on Scenario 12 (S12).

Table 5
Scenarios performance indexes in a cloudy sky day.

Scenario	IAE_{C1} [°Ch]	$NCAE_f$	$NCAE_q$	N_{fs}	BT	IAE_{C2} [°Ch]	$NCAE_v$	t_{op} [h]	E_{evap} [MJ]	X_{evap} [MJ]
S7	1.51×10^5	132.16	2.40	0	1	1.16×10^4	24.00	4.36	−315.89	16.79
S8	1.49×10^5	0.00	120.78	40	0	1.46×10^3	58.00	5.73	−605.86	30.93
S9	1.24×10^5	134.80	101.36	3	0	3.09×10^2	62.00	5.94	−564.86	28.79
S10	1.21×10^5	35.17	2.40	0	0	1.30×10^3	1.63	5.68	−523.01	27.44
S11	1.42×10^5	0.00	107.17	39	0	1.38×10^4	9.54	6.13	−663.25	34.58
S12	1.07×10^5	11.84	10.13	0	0	2.09×10^3	2.06	6.05	−608.53	31.69

19:00, the flow saturates at maximum, and C1 manipulates the focus, reducing it to reject the irradiance disturbances. Note in Fig. 8.a that the T_2 steadily follows the set-point despite the strong irradiance disturbances of irradiance (yellow lin) in Fig. 8.c.

Table 5 depicts scenarios S7 to S12 regarding cloudy sky irradiation cases. In this case, columns N_{fs} and *BT* of Table 5 show that no controller evaluated in scenarios S7, S8, and S9 is suitable to operate the absorption plant without burning gas and avoiding safety complete defocus events. All simulations from S10 to S12 do not start the gas boiler, although Scenario S11 presents safety full defocus events. The defocus action shows that the PI law in C2 alone cannot avoid overheating for a cloudy sky scenario. Interestingly, the revamp controller simulated on scenario S11 presents the best energy and exergy production of Table 5. This production occurs because the plant operates at a higher temperature for an extended period. Since Equation (15) and Equation (16) describe the energy and exergy production, the higher temperature, the higher the production. This operation is undesirable once the energy production enhancement results from an abnormal dangerous overheating condition that degrades the equipment.

Again the controllers of scenarios S10 and S12 are the only ones capable of operating the plant without triggering the gas burner and avoiding safety full defocus events. Compare the S10 and S12 performance indexes compiled in Table 5. The controller performance on simulation S10 leads to −523.01[*MJ*] and 27.44[*MJ*] of energy and exergy production, while the proposed controllers on simulation S12 produce − 608.53[*MJ*] and 31.69[*MJ*] of cooling energy and exergy, respectively. Therefore, the proposed controllers increase 16% of cooling energy production and 15% of exergy production compared to S10. The production increase follows an IAE_T reduction of 12% and an $NCAE_T$ reduction of 39%.

6. Conclusion

The proposed Fresnel split-range and HTG PI controllers enable operating the EITS solar absorption plant avoiding gas burning, and safety defocus events. While the absorption chiller PI controller drastically reduces plant oscillations and actuators' effort, the split-range controller accelerates plant start-up with overheat prevention, enhanced stability, and increased production. The split-range control sums the advantages of manipulating the flow and focus in a simple, well-known, yet powerful control technique. As far as the authors know, this is the first application of a split-range advanced control technique in a line focus solar collector. For future works, it would be interesting to apply this control in the actual plant to evaluate its performance, and to develop a systematic split-range controller design approach to generalize its use in concentrating solar collectors.

CRediT authorship contribution statement

Diogo Ortiz Machado: Conceptualization, Investigation, Writing – original draft. **Adolfo J. Sánchez:** Conceptualization, Investigation, Writing – original draft. **Antonio J. Gallego:** Conceptualization, Software, Resources. **Gustavo A. de Andrade:** Software, Writing – review & editing, Supervision, Writing – review & editing. **Julio E. Normey-Rico:** Project administration, Resources, Supervision, Writing – review & editing. **Carlos Bordons:** Project administration, Resources, Supervision, Writing – review & editing. **Eduardo F. Camacho:** Writing – review & editing.

Declaration of competing interest

The authors declare that they have no known competing financial interests or personal relationships that could have appeared to influence the work reported in this paper.

Acknowledgement

The authors would like to acknowledge the Coordenação de Aperfeiçoamento de Pessoal de Nível Superior (CAPES), Finance Code 001, the Conselho Nacional de Desenvolvimento Científico e Tecnológico (CNPq), under grant 304032/2019–0, the Agencia Estatal de Investigación (AEI) of the Spanish Ministry of Science and Innovation, under grant PID2019-104149RB-I00/10.13039/501100011033 (project SAFEMPC), and the European Research Council under Advanced Research Grant OCONTSOLAR (789051), for funding this work. Diogo O. Machado thanks to IFRS- campus Rio Grande for capacity support, *Fundación Carolina*, SEGIB and PrInt-UFSC programms for mobility scholarships.

References

[1] C. Heeckt, S. Kolaric, Urban Sustainability in Europe: what Is Driving Cities' Environmental Changes?, Tech. rep., European Environment Agency. URL https://www.eea.europa.eu/publications/urban-sustainability-in-europe-what.
[2] M.J. Blanco, L.R. Santigosa, Advances in Concentrating Solar Thermal Research and Technology, first ed., Woodhead Publishing, 2017.
[3] European Commission, Communication of the commission to the european parliament and the council concerning the paris protocol- a blueprint for tackling global climate change beyond 2020, URL, https://ec.europa.eu/info/publications/paris-protocol-blueprint-tackling-global-climate-change-beyond-2020, 2015.
[4] E. Commission, Climate action. paris agreement, URL, https://ec.europa.eu/clima/eu-action/international-action-climate-change/climate-negotiations/paris-agreement_en, 2015.
[5] N. Engineering, National academy of engineering. grand challenges for engineering, URL, www.engineeringchallenges.org, 2008.
[6] A.J. Gallego, A.J. Sánchez, M. Berenguel, E.F. Camacho, Adaptive ukf-based model predictive control of a fresnel collector field, J. Process Control 85 (2020) 76–90.
[7] R. Meligy, M. Rady, A.E. Samahy, W. Mohamed, Proportional–integral-like fuzzy controller of a small-scale linear fresnel reflector solar plant, IET Renew. Power Gener. 14 (8) (2020) 2620–2628.
[8] E. F. Camacho, A. J. Gallego, J. M. Escaño, A. J. Sánchez, Hybrid nonlinear MPC of a solar cooling plant, Energies 12 (14). doi:10.3390/en12142723.
[9] C. Marugán-Cruz, D. Serrano, J. Gómez-Hernández, S. Sánchez-Delgado, Solar multiple optimization of a dsg linear fresnel power plant, Energy Convers. Manag. 184 (2019) 571–580.
[10] M.J. Montes, A. Abánades, J.M. Martínez-Val, M. Valdés, Solar multiple optimization for a solar-only thermal power plant, using oil as heat transfer fluid in the parabolic trough collectors, Sol. Energy 83 (12) (2009) 2165–2176, https://doi.org/10.1016/j.solener.2009.08.010.
[11] D. Machado, J.E. Normey-Rico, G.A. de Andrade, A 2dof thermosolar concentrator proposal: solar tracking and disturbance rejection using proportional

defocus, in: ISES Solar World Congress SWC 2019, International Solar Energy Society, 2019, pp. 34–41, https://doi.org/10.18086/swc.2019.01.05. URL.
[12] P. Bermejo, F.J. Pino, F. Rosa, Solar absorption cooling plant in Seville, Sol. Energy 84 (8) (2010) 1503–1512, https://doi.org/10.1016/j.solener.2010.05.012.
[13] Mercado Iberico Del Gas, Natural gas prices, URL, https://www.mibgas.es/en, 2021.
[14] Red Electrica España, Electric energy cost, URL, https://www.ree.es/es/accionistas-e-inversores/la-accion/red-electrica-en-bolsa, 2021.
[15] J. Morud, S. Skogestad, Effects of recycle on dynamics and control of chemical processing plants, Comput. Chem. Eng. 18 (1994) S529–S534, https://doi.org/10.1016/0098-1354(94)80086-3. URL.
[16] W.L. Luyben, Dynamics and control of recycle systems. 1. Simple open-loop and closed-loop systems, Ind. Eng. Chem. Res. 32 (3) (1993) 466–475, https://doi.org/10.1021/ie00015a010.
[17] W.L. Luyben, Dynamics and control of recycle systems. 3. Alternative process designs in a ternary system, Ind. Eng. Chem. Res. 32 (6) (1993) 1142–1153, https://doi.org/10.1021/ie00018a020.
[18] J.E. Normey-Rico, E.F. Camacho, Control of Dead-Time Processes, Springer, 2007.
[19] E. Camacho, M. Berenguel, F.R. Rubio, D. Martínez, Control of Solar Energy Systems, Springer London, Dordrecht Heidelberg New York, 2006, https://doi.org/10.1007/978-0-85729-916-1.
[20] A.J. Gallego, G.M. Merello, M. Berenguel, E.F. Camacho, Gain-scheduling model predictive control of a Fresnel collector field, Control Eng. Pract. 82 (2019) 1–13, https://doi.org/10.1016/j.conengprac.2018.09.022. URL.
[21] M.V. Robledo, Description and Commissioning of a Solar Absorption Refrigeration Plant. Modeling and Control of the Fresnel Solar Collector (in spanish), Ph.D. thesis, Universidad de Sevilla, 2012. URL, http://bibing.us.es/proyectos/abreproy/12074.
[22] A. Reyes-Lúa, C. Zotică, K. Forsman, S. Skogestad, Systematic design of split range controllers, IFAC-PapersOnLine 52 (1) (2019) 898–903, https://doi.org/10.1016/J.IFACOL.2019.06.176.
[23] M. Bartyś, B. Hryniewicki, The trade-off between the controller effort and control quality on example of an electro-pneumatic final control element, 2019, Actuators 8 (1) (2019) 23, https://doi.org/10.3390/ACT8010023. URL, https://www.mdpi.com/2076-0825/8/1/23/htmhttps://www.mdpi.com/2076-0825/8/1/23.
[24] M.J. Moran, H.N. Shapiro, Fundamentals of Engineering Thermodynamics, fifth ed., John Wiley & Sons, 2006 https://doi.org/10.1038/1811028b0. http://www.nature.com/doifinder/10.1038/1811028b0.
[25] IEA ECBCS, "Annex 49: low exergy system for high-performance building and communities" Stuttgart, Germany, Fraunhofer Verlag, 2011. Available online: www.annex49.com. (Accessed 22 March 2020).
[26] M. Virtanen, J. Palmer, Heating and Cooling with a Focus on Increased Energy Efficiency and Improved Comfort ECBCS Annex 37 Project Summary Report, AECOM Ltd on behalf of the International Energy Agency, 2010. URL, www.ecbcs.org.